8 Spectral diffusion and mechanism for autodissociation

We study the spectral response of the transition between the first and the second excited state of the O–H stretch vibration of HDO dissolved in liquid D_2O with two-color femtosecond mid-infrared spectroscopy. The spectral response of this transition differs strongly from the fundamental absorption spectrum of the O–H stretch vibration. In addition, excitation of the O–H stretch vibration is observed to lead to a change of the hydrogen-bond dynamics of liquid water. We show that both these observations can be described with a refined quantum-mechanical version of the Lippincott-Schroeder model for hydrogen-bonded OH$\cdots$O systems. An important implication is that excitation of the $v = 2$ state of the OH stretch vibration can initiate the autodissociation reaction $2H_2O \rightarrow H_3O^+ + OH^-$.

8.1 Introduction

In the previous chapters, we saw that the hydrogen bonds in liquid water,

$$HO{-}H\cdots OH_2,$$

or the equivalent in the isotopically labeled HDO:D_2O solution, are not static, but undergo fluctuations around their equilibrium length on a time scale of about one picosecond. Since separating two hydrogen-bonded water molecules requires energy, these length fluctuations are bounded by the available thermal energy at a given temperature. We have modeled these dynamics by assuming that the length fluctuations can be interpreted as diffusion of a particle in a parabolic potential, that represents the energy of the OH$\cdots$O system $W(R)$ as a function of the hydrogen-bond length R, defined as the O$\cdots$O distance (about 2.85 Å in water). These potentials $W_v(R)$ for vibrational states $v = 0, 1, 2$ were shown schematically in Fig. 5.3, with the roles of D and H swapped. The assumption of a parabolic, or harmonic, potential is justified, since the typical thermal energy is $k_B T \approx 207$ cm^{-1}, while the dissociation energy of the hydrogen bond is around 1900 cm^{-1} (23 kJ/mol). As a probe for the hydrogen-bond length, we use the OH stretch vibration in an HDO molecule, whose frequency depends parametrically on R. The fact that the OH stretch mode has discrete ground and excited states implies that it must be described quantum-mechanically. In this description, each vibrational state corresponds to a solution of the Schrödinger equation that describes the probability amplitude of the proton (the nucleus of the H atom) as a function of the proton coordinate r (defined as the O$-$H distance), with a potential energy $V(r, R)$. For $R \rightarrow \infty$, this potential has a shape similar to the curve shown in Fig. 2.6, for which a harmonic potential with a small anharmonic correction is a good approximation for the lowest few vibrational states. However, the potential $V(r, R)$ is obviously different for the typical value $R \approx 2.8$ Å: it must go to infinity

for $r \to R$. Such a strong anharmonicity must affect even the lowest vibrational states of the OH stretch vibration. We will relate this anharmonicity to the shape of the transient spectrum of vibrationally excited HDO molecules and refine the description of spectral diffusion (Ref. 129 and §5.4). Finally, we will discuss the implications of the anharmonicity of the OH stretch mode on the autodissociation reaction $2H_2O \to H_3O^+ + OH^-$.

8.2 EXPERIMENT

The experiments were pump–probe measurements where a femtosecond infrared laser pulse excited the $v = 0 \to 1$ transition of the OH stretch vibration of HDO molecules dissolved in D_2O. The sample consists of a 200 μm-thick layer of HDO dissolved in D_2O with a transmittance of approximately 5% at 3400 cm^{-1}, the center of the $v = 0 \to 1$ absorption band. The sample was at room temperature and at a fixed position in the laser beam focus (see §2.8 for an estimate of the accumulated heat) Apart from the sample, the setup is identical to the setup described in §6.2, which yielded the absorbance change $\Delta\alpha(\omega_{pr}, t)$ for a fixed pump frequency of 3420 cm^{-1} and a range of probe frequencies ω_{pr} and pump–probe delays t.

8.3 THE EQUILIBRATED TRANSIENT SPECTRUM

We saw in Chapter 5 that the spectral correlation time for the OD stretch vibration is 400 fs, which is a measure for the solvent relaxation time. For the OH stretch vibration of HDO in D_2O, other studies[33,36,129] showed spectral relaxation times of 0.5 and 0.7 ps, which means that after 1–2 ps, the distributions of the hydrogen-bond lengths for populations in the $v = 0$ and $v = 1$ states will have nearly equilibrated within the $W_0(R)$ and $W_1(R)$ potentials, respectively. At these larger delays, the transient spectrum decreases in amplitude due to vibrational relaxation, but does not change its shape significantly. Figure 8.1 presents transient absorption spectra of the OH stretch vibration delays of 0.5, 1, and 2 ps for a pump spectrum centered at 3420 cm^{-1}.

For probe frequencies >3300 cm^{-1}, the signal is positive and results from the bleaching of the $v = 0 \to 1$ transition. For frequencies <3300 cm^{-1}, the signal is negative and results from the induced $v = 1 \to 2$ absorption. For both pump frequencies, the width of the bleaching band increases with the pump–probe delay, which indicates a spectral hole that broadens due to spectral relaxation. Because of the relation between the hydrogen-bond length R and the vibrational frequency ω (§1.1), we see here directly how the initial narrow distribution of hydrogen-bond lengths that was selected by the spectrum of the pump pulse broadens in time due to the rapid length fluctuations.

At larger delays t, the bleaching has the nearly-Gaussian shape of the linear absorption spectrum in Fig. 1.3. In contrast, the spectral shape of the $v = 1 \to 2$ absorption is much broader and much steeper on the high-frequency side than on the low-frequency side. The steep high-frequency side can partly be explained from the cancellation of the bleaching and the induced absorption in this frequency region. However, even after correction for this effect, the resulting induced absorption remains strongly asymmetric. The asymmetryand the width of the $v = 1 \to 2$ band are surprising, because the anharmonicity at the

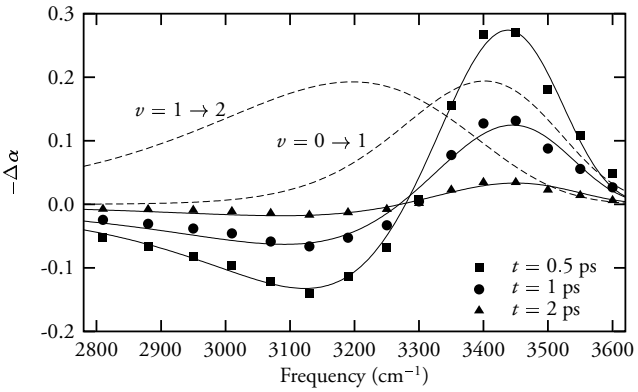

FIGURE 8.1. Transient spectra of HDO dissolved in D_2O after excitation of the OH stretch mode at 3420 cm^{-1}, for three pump–probe delays t. The solid curves represent transient spectra that are calculated with the modified quantum-mechanical Lippincott-Schroeder (QLS) model (§8.3.1). The dashed curves represent calculated absorption spectra for the $v = 0 \rightarrow 1$ and $v = 1 \rightarrow 2$ transitions in thermal equilibrium.

lowest vibrational levels is normally small for strong chemical bonds,[95] such as the CO stretch,[1,49,94] the CH stretch,[120] and even the weakly hydrogen-bonded OD stretch.[5]

8.3.1 QUANTUM-MECHANICAL LIPPINCOTT-SCHROEDER MODEL

The assumption of harmonic hydrogen-bond potentials $W(R)$, mentioned in §8.1, results in a Gaussian-shaped linear absorption spectrum, in quite good agreement with the empirical linear OH-stretch spectrum of HDO in D_2O (Fig. 1.3). A correlation-function approach[8,9] yields similar spectra. However, from Fig. 8.1, it is clear that the $v = 1 \rightarrow 2$ absorption spectrum has a strongly non-Gaussian shape that cannot be accounted for by the Brownian oscillator model. The description of the $v = 1 \rightarrow 2$ absorption spectrum requires a more advanced model that, in contrast to the Brownian oscillator model, includes strong anharmonicities for the potentials of the OH stretch and the OH$\cdots$O hydrogen-bond coordinates.

As a starting point for a description of the anharmonic coupling between the OH stretch vibration and the hydrogen-bond mode, we use the so-called Lippincott-Schroeder (LS) model.[73] This model is based on the empirical correlation between the frequency of the OH stretch vibration and the length of the OH$\cdots$O hydrogen bond R (§1.1). This correlation is surprisingly similar for systems that differ in the strength of local electric fields and in the presence of other interaction than the hydrogen bond. This universal behavior can be explained from the fact that most interactions affect the OH stretch mode of a hydrogen-bonded system mainly by changing the length of the polarizable OH$\cdots$O hydrogen bond. These interactions thus have very little effect on the relation between the OH stretch vibration and the OH$\cdots$O hydrogen bond, and mainly express themselves in a change of the length of this bond. Hence, the interactions between the OH stretch mode of the HDO molecule and its surroundings is well approximated with a single well-defined relation between the vibrational potential $V(r, R)$ and the hydrogen-bond length

R. Such a relation is provided by the LS model.

We write the potential energy $V(r,R) = V_{\rm I}(r,R) + V_{\rm II}(R)$ as the sum of two terms. The first term is the original LS potential,[73]

$$V_{\rm I}(r,R) = D_{\rm Ia}\left[1 - e^{-n_{\rm Ia}(r-r_o)^2/2r}\right] + D_{\rm Ib}\left[1 - e^{-n_{\rm Ib}(R-r-r_o)^2/2(R-r)}\right]. \tag{8.1}$$

The parameters of $V_{\rm I}(r,R)$ follow from various known parameters. The energy $D_{\rm Ia} = 38750$ cm^{-1} is the binding energy of the OH bond of water (463 kJ/mol), $n_{\rm Ia} = 9.8$ Å^{-1} defines the frequency of the OH stretch vibration, $r_o = 0.97$ Å is the OH bond length in the gas phase (absence of a hydrogen bond), and $D_{\rm Ib}$ is determined by the empirical relations between r, R, and the OH stretch frequency. An excellent description of these relations is obtained with $D_{\rm Ia}/D_{\rm Ib} \approx 1.5$.[73] Here we use $D_{\rm Ib} = 25000$ cm^{-1}. The validity of the LS model has been supported by a quantum-mechanical calculation[76] of $V_{\rm I}(r,R)$ for the $H_5O_2^-$ ion, that showed behavior similar to the Lippincott-Schroeder potential.

In the past, the LS model has mostly been used classically. Only more recently, the model was used quantum-mechanically to calculate the vibrational lifetime of the OH stretch vibration.[114] In the original treatment, the frequency of the OH stretch vibration was calculated from a harmonic approximation around the minimum of $V_{\rm I}$. Clearly, this procedure cannot account for the anharmonicity that causes the lower frequency of the $v = 1 \rightarrow 2$ transition compared to the $v = 0 \rightarrow 1$ transition. Therefore, we perform a quantum-mechanical calculation by solving the one-dimensional Schrödinger equation for the OH coordinate r in the LS potential $V_{\rm I}(r,R)$. We will refer to this quantum-mechanical LS model as the QLS model.

We use an adiabatic approximation with R as a parameter, which implies that the first and second derivative of the vibrational wavefunctions of the OH stretch vibration with respect to R are neglected. This type of adiabatic approach is commonly used in describing the coupling between a high-frequency OH stretch vibration and a low-frequency OH$\cdots$O hydrogen bond.[7,82] We used the Numerov method[19] to calculate the vibrational eigenfunctions $\phi_v(r,R)$ as a function of R for all states v. The eigenfunctions have energies $E_v(R)$. The adiabatic approximation will be valid if the motion in R is much slower than that in r. The corresponding characteristic frequencies of 200 cm^{-1} (hydrogen-bond vibration)[47] and 3400 cm^{-1} (OH stretch) are sufficiently different to justify this approximation. This approximation implies that eigenstates of the entire O–H$\cdots$O system are product states $\phi_v(r,R)\psi_{v'}(R)$, where v' is the (possibly high) hydrogen-bond quantum number and v is the OH stretch quantum number (0, 1, or 2). Without the adiabatic approximation, these product states would not be not pure eigenstates, with the result that an excited OH stretch state ($v = 1$) decays to its ground state ($v = 0$), during which the energy is transfered to the hydrogen-bond mode. In other words, the adiabatic approach does not describe vibrational relaxation, which was discussed in Chapter 4 (see especially Fig. 4.5).

In $V_{\rm I}$, the original LS potential, R was treated as an externally imposed parameter, i.e. the distance two molecules happened to have in a solution. The second potential term, $V_{\rm II}(R)$, is necessary to describe the electrostatic attraction of two water molecules at large distances and their repulsion at short distances. Such an attraction can usually be described by the Morse potential

$$V_{\rm II}(R) = D_{\rm II}\left[1 - e^{-n_{\rm II}(R-R_o)}\right]^2. \tag{8.2}$$

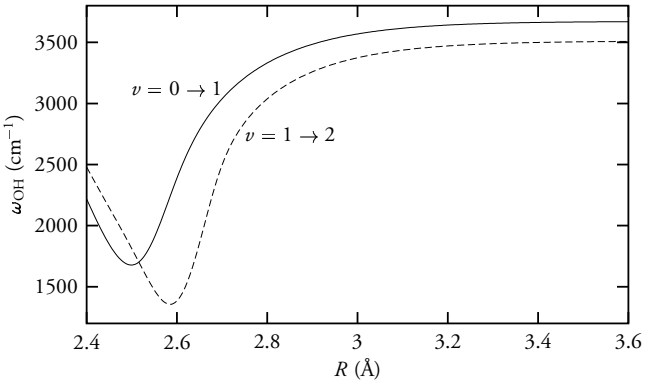

FIGURE 8.2. Frequencies of the $v = 0 \rightarrow 1$ and the $v = 1 \rightarrow 2$ transitions as a function of the oxygen-oxygen distance R of the OH$\cdots$O hydrogen bond, calculated with the QLS model (§8.3.1).

However, $V_{II}(R)$ is not yet equivalent to the hydrogen-bond potential $W_v(R)$, because the latter involves the energy $E_v(R)$ of the OH stretch vibration state v as well. Thus, $W_v(R) = E_v(R) + V_{II}(R)$. The yet unknown parameters in the potentials V_I and V_{II} are now n_{Ib} [Eq. (8.1)], D_{II}, n_{II}, and R_o. Since the potential $W_o(R)$ for the vibrational ground state must describe the empirical values[25] for the hydrogen-bond dissociation energy (1900 cm^{-1}), the equilibrium length $R_{eq,o} = 2.85$ Å, and the hydrogen-bond stretch frequency of $\sim$200 cm^{-1} (Ref. 47), there is effectively only one independent parameter left that must be determined from a fit to the transient spectra in Fig. 8.1 (details follow in §8.3.2). We find: $n_{Ib} = 16.5(1.0)$ Å^{-1}, $D_{II} = 2000$ cm^{-1}, $n_{II} = 2.9(2)$ Å^{-1}, and $R_o = 2.88$ cm^{-1}. We note that the values for D_{II} and R_o affect the transient spectra only weakly. However, the values of n_{Ib} and n_{II} have a strong effect on the transient spectra. The asymmetry of the $v = 0 \rightarrow 1$ and $v = 1 \rightarrow 2$ absorption bands is strongly determined by n_{Ib}, and the width of these bands depends on n_{II}.

The transition $v = i \rightarrow j$ has an associated frequency $\omega_{ij}(R) = [W_j(R) - W_i(R)]/\hbar$ as a function of the oxygen-oxygen distance R. Figure 8.2 shows the calculated frequencies $\omega_{01}(R)$ and $\omega_{12}(R)$. The calculated $\omega_{01}(R)$ shows a strongly nonlinear dependence on R, in good agreement with experimental observations.[85,92] Figure 8.3 shows the hydrogen-bond potentials $W_o(R)$, $W_1(R)$ and $W_2(R)$ (corresponding to $v = 0, 1, 2$ states), together with the V_I potential.

The origin of the large width and asymmetric shape of the $v = 1 \rightarrow 2$ absorption spectrum is the change of the distribution in R upon excitation of the OH stretch vibration. We find that the equilibrium lengths $R_{eq,v}$ of the hydrogen bond decreases with increasing quantum number v of the OH stretch mode: $R_{eq,o} = 2.85$ Å, $R_{eq,1} = 2.80$ Å, and $R_{eq,2} = 2.70$ Å. The derivatives $d\omega_{01}/dR$ and $d\omega_{12}/dR$ of the $v = 0 \rightarrow 1$ and $v = 1 \rightarrow 2$ transitions are largest for smaller R, as can be seen from Fig. 8.2. Hence, a given distribution of R results in a $v = 1 \rightarrow 2$ spectrum that is broader than the $v = 0 \rightarrow 1$ spectrum. For R in the range 2.6–2.9 Å, which corresponds to the thermal distribution in the $v = 1$ state, the derivative $d\omega_{12}/dR$ is very large. We can understand the latter from the shape of the r-dependent potential-energy contribution $V_I(r, R)$. Figure 8.4 shows the poten-

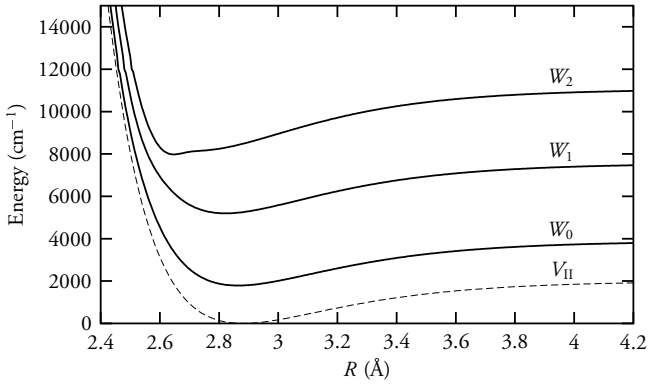

FIGURE 8.3. Hydrogen-bond potentials $W_v(R)$ for the $v = 0, 1, 2$ states of the OH stretch mode, together with the Morse potential $V_{II}(R)$. These functions are obtained by fitting the parameters of the QLS model (§8.3.1) to the transient spectra in Fig. 8.1.

tial $V_I(r, R)$ as a function of the OH bond length for a few values of the oxygen-oxygen distance R.

At oxygen-oxygen distances R below 2.7 Å, the potential $V_I(r, R)$ becomes very broad at the $v = 2$ energy level. This broadening of the potential leads to a strongly delocalized $v = 2$ state and a decrease of E_2. Hence, in this region of R, a small variation in R leads to a large change of E_2. As a result, the transition frequency of the $v = 1 \rightarrow 2$ transition varies strongly over the thermal distribution of R (with a width of ≈ 0.36 Å at 300 K), which leads to a strong broadening of the $v = 1 \rightarrow 2$ transition. The delocalization of the $v = 2$ state for $R \leq 2.7$ Å also affects the shape of the $v = 0 \rightarrow 2$ overtone transition of the OH stretch vibration. This overtone spectrum has been extensively studied for different isotopes of ice[61,107] and water.[71] For water, the $v = 0 \rightarrow 2$ overtone transition is indeed strongly asymmetrically broadened to lower frequencies,[71] similar to the $v = 1 \rightarrow 2$ transition in Fig. 8.1.

8.3.2 CALCULATION OF TRANSIENT SPECTRA

To calculate the transient spectra, we evaluated the potentials $W_v(R)$ numerically for R in the range 2.2–3.8 Å with a step size $\delta R = 0.004$ Å. For every value of R, we calculated the transition dipole matrix elements

$$\mu_{01}(R) = \langle \phi_1(r, R)|r|\phi_0(r, R)\rangle_r, \tag{8.3}$$

$$\mu_{12}(R) = \langle \phi_2(r, R)|r|\phi_1(r, R)\rangle_r, \tag{8.4}$$

that represent the probabilities for the $v = 0 \rightarrow 1$ and $v = 1 \rightarrow 2$ transitions at a given value of R. The subscript r indicates that the integration should be carried over r. We assume that at larger delays after the pump pulse, the population $\Delta n_1(R)$ of the $v = 1$ state and the population depletion $-\Delta n_0(R)$ are thermal distributions

$$\Delta n_0(R) = N_0 e^{-\beta W_0(R)}, \tag{8.5}$$

$$-\Delta n_1(R) = N_1 e^{-\beta W_1(R)}, \tag{8.6}$$

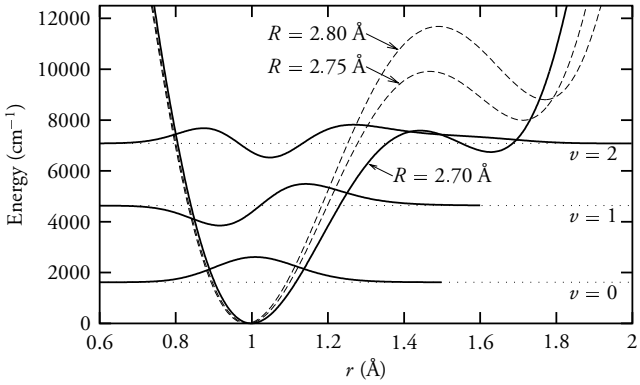

FIGURE 8.4. Vibrational potential V_1 for three different oxygen-oxygen distances R of the OH$\cdots$O hydrogen bond as a function of the OH bond length r. Also shown are the vibrational wavefunctions of the $v = 0, 1, 2$ states for $R = 2.7$ Å.

where N_v are normalization factors such that

$$\int \Delta n_0(R)dR = -\int \Delta n_1(R)dR = 1. \tag{8.7}$$

and $\beta = 1/k_B T$. If we denote the inverse function of $\omega_{ij}(R)$ by $R_{ij}(\omega)$, the frequency spectrum is given by

$$\begin{aligned} -\Delta\tilde{\alpha}(\omega) \quad \propto \quad & \left[\Delta n_0(R_{01}) + \Delta n_1(R_{01})\right] \cdot \left|\mu_{01}(R_{01})\right|^2 \cdot \frac{dR_{01}}{d\omega} \\ & + \Delta n_1(R_{12}) \cdot \left|\mu_{12}(R_{01})\right|^2 \cdot \frac{dR_{12}}{d\omega}. \end{aligned} \tag{8.8}$$

The derivatives of R_{ij} are necessary to transform the distribution $n_i(R_{ij})$ (particles per unit of R_{ij}) to the distribution $\Delta\tilde{\alpha}(\omega)$ (absorption per unit of ω). The above equation is in fact nothing more than a precise version of Eq. (5.4) and Eq. (7.28). To translate this frequency spectrum to the observed transient spectrum $\Delta\alpha(\omega)$ (Fig. 8.1), a convolution with the effective probe spectrum $F_{pr}(\omega')$ is necessary (see also §2.6):

$$\Delta\alpha(\omega) = \bar{\sigma} \int d\omega' \, \Delta\tilde{\alpha}(\omega - \omega') \, F_{pr}(\omega'), \tag{8.9}$$

where $\bar{\sigma}$ defines the amplitude of the bleaching [see also Eq. (1.6)] and $F_{pr}(\omega)$ is the convolution of the probe pulse spectrum and a homogeneous line shape with an FWHM of 90 cm^{-1}. We will discuss the homogeneous line shape in §8.4, where we also discuss the effect of the equilibration process on the transient spectrum.

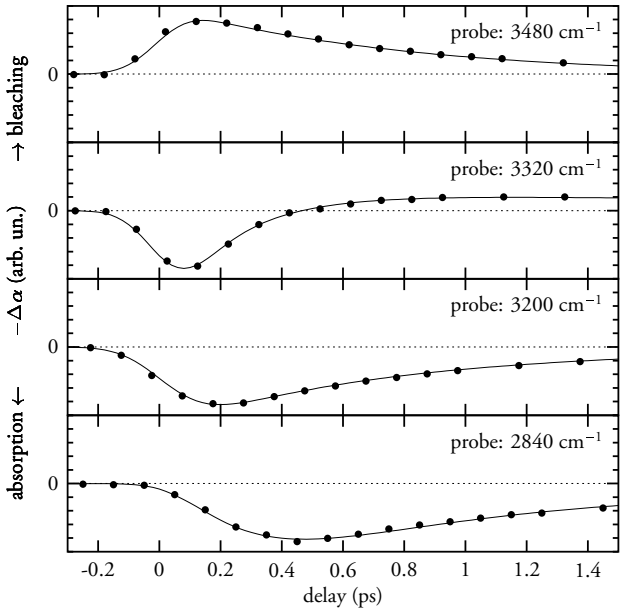

FIGURE 8.5. Pump–probe delayscans of HDO:D_2O after excitation of the OH stretch mode at 3560 cm^{-1}. The drawn lines result from the QLS model in combination with the spectral dynamics discussed in §8.4.1 and §8.4.2.

8.4 THE DYNAMICS OF THE TRANSIENT SPECTRA

8.4.1 SPECTRAL DIFFUSION

The transient spectra in Fig. 8.1, taken at pump–probe delays $t > 0.5$ ps, differ mainly in amplitude. For shorter delays, this is no longer true. Figure 8.5 shows pump–probe delayscans after excitation at 3560 cm^{-1}. Especially the data where the probe frequency was 2840 cm^{-1} shows a response directly after excitation (delay $t = 0$) that is significantly slower than in the data where the probe frequency was 3320 cm^{-1}. This delayed response results from spectral dynamics.

Because of the strong overdamped behavior of the hydrogen bond (§4.5), we describe the hydrogen-bond dynamics as a classical diffusive process in the $W_0(R)$ and $W_1(R)$ hydrogen-bond potentials. In Chapters 5, 6, and 7, we approximated the hydrogen-bond potentials by harmonic potentials, for which the diffusive hydrogen-bond dynamics could be described analytically. However, in order to take the strong anharmonicity of the potentials $W_v(R)$ (Fig. 8.4) fully into account, a numerical calculation is necessary. In related previous microscopic semiclassical treatments, the dynamics on the potential-energy surfaces of the ground and excited state were calculated using molecular dynamics simulations.[14,83,32] Here, we describe the dynamics of the hydrogen bonds as a diffusion process in a potential well $W_v(R)$. The populations $\Delta n_v(R)$ discussed in the previous section are created by a pump pulse. Directly after excitation ($t = 0$), the distributions of the

population changes are

$$\Delta n_1(R) = -\Delta n_0(R) = F_{\mathrm{pu}}(\omega_{01}(R)) \cdot |\mu_{01}(R)|^2 \cdot \frac{d\omega_{01}}{dR}, \tag{8.10}$$

where $F_{\mathrm{pu}}(\omega)$ is the pump-pulse spectrum, convolved with the homogeneous linewidth (§2.6) that has an FWHM of 90 cm^{-1}. This homogeneous broadening is necessary to describe the shape of the transient spectra around $t = 0$, when the broadening effect of spectral diffusion is still limited. In a recent publication,[115] a similar homogeneous linewidth in HDO:D_2O was observed by means of photon-echo experiments on the OH stretch vibration. After excitation, the distributions $\Delta n_v(R, t)$ satisfy the diffusion equation[63]

$$\frac{\partial \Delta n_v}{\partial t} = \frac{L_v^2}{\tau_{\mathrm{D}}} \left(\frac{\partial^2 \Delta n_v}{\partial R^2} + \beta \Delta n_v \frac{d^2 W_v}{dR^2} + \beta \frac{\partial \Delta n_v}{\partial R} \frac{dW_v}{\partial R} \right), \tag{8.11}$$

where L_v is the half-width at $e^{-1/2}$ of the maximum of the equilibrium distribution in the potential $W_v(R)$, and τ_{D} is the characteristic time scale for the diffusion process. For a system with harmonic potentials and Gaussian-shaped spectra, the spectral diffusion can be described by the autocorrelation function in Eq. (5.3); the spectral correlation time τ_{c} is exactly the same as τ_{D} in Eq. (8.11). Its value can be determined from the time dependence of the first moment of the transient spectrum [see Eq. (5.10)], from which a value of 700 fs follows.[33] For non-parabolic hydrogen-bond potentials, the first moment of the transient spectrum depends has no longer an exponential time dependence. However, we find that for the present hydrogen-bond potentials $W_v(R)$, the value of τ_{c}, as it can be determined from the delay dependence of the calculated first spectral moment, differs negligibly from τ_{D}. In the following, we will therefore use $\tau_{\mathrm{D}} = \tau_{\mathrm{c}} = 700$ fs. We solved Eq. (8.11) numerically by discretizing the R and t in steps $\delta R = 0.004$ Å and $\delta t = 2$ fs, respectively (see §7.6.4 for details). According to this diffusion equation, the populations Δn will evolve towards the thermal distribution discussed in §8.3.2. To translate the resulting time-dependent $\Delta n_v(\omega, t)$ to the transient spectrum, we use Eq. (8.9) for $t \geq 0$, which we convolve with the pump–probe cross-correlate, with a duration of 300 fs FWHM (§2.6).

The above modeling of spectral diffusion describes the hydrogen-bond dynamics in the adiabatic approximation, in which no transitions from the $v = 1$ to the $v = 0$ population are possible. Non-adiabatic transitions, or vibrational relaxation, are likely to have a strong impact on the hydrogen-bond dynamics, since the released vibrational energy is converted to to kinetic energy of the hydrogen-bond motion. However, vibrational relaxation of an OH oscillator also implies that the latter has returned to the vibrational ground state, where it no longer contributes to the $v = 0 \rightarrow 1$ and $v = 1 \rightarrow 2$ bands in the transient spectrum. Thus, the hydrogen-bond dynamics observed in the transient spectra are the result of purely adiabatic dynamics, i.e. the dynamics of those oscillators that do not undergo vibrational relaxation. We note here that the excitation of the hydrogen bond accompanying the vibrational relaxation causes a measurable temporary blueshift of the relaxed OH stretch vibration, as we saw in Chapter 4. This blueshift may affect the transient spectrum to a small extent, but we neglected it in the present analysis.

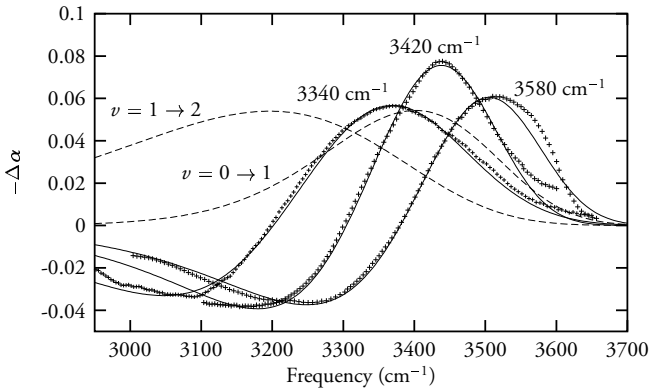

FIGURE 8.6. Transient spectra of HDO:D_2O, pumped at three different frequencies, at delay t = 0.30 ps. Data points: experiment (by Gallot and co-workers[33,35]); drawn curves: QLS model; dashed curves: equilibrated spectra of $0 \rightarrow 1$ and $1 \rightarrow 2$ transitions of the OH band.

8.4.2 INERTIAL DYNAMICS

Because the time resolution is limited by the pump–probe cross-correlation function (with its 300 fs FWHM duration), the data in Fig. 8.1 do not display spectral relaxation very clearly. However, Gallot and co-workers have performed similar experiments[33,35] with a better time resolution (cross-correlate 210 fs) and have kindly placed their data at our disposal. In their data, the broadening and the shift of the bleaching band are very clearly visible. However, the modeling of the hydrogen-bond dynamics with a single diffusive process does not provide a good description of Gallot's data, especially in the region of the $v = 1 \rightarrow 2$ transition. This is illustrated in Fig. 8.8, which shows the frequency at which the induced absorption changes into a bleaching as a function of delay. The pump frequency was 3580 cm^{-1}. The experimentally observed frequencies are compared with the results of two calculations in which the hydrogen-bond dynamics is purely diffusive. At short delay times ($t < 500$ fs), the experimentally observed zero-crossings can be fitted well with a fast diffusion process with a time constant $\tau_c = 600$ fs, but for longer delay times (>1 ps), this value describes the experimental data poorly. At these longer delay times, a much better description is obtained with $\tau_c = 950$ fs. Hence, during the first 500 fs after excitation, the transient spectra show a rapid shift towards lower frequencies. This rapid shift is followed by a much slower evolution to the final thermal distribution.

The fast process during the first 500 fs is more pronounced at frequencies <3450 cm^{-1} than at frequencies >3550 cm^{-1} in the transient spectra in Ref. 35, which indicates that the fast process has a much stronger effect on the $v = 1 \rightarrow 2$ induced absorption spectrum than on the $v = 0 \rightarrow 1$ bleaching signal. This observation suggests that the fast process only affects the $v = 1$ state. The solid curves in Figs. 8.1 and 8.8 represent the results of a calculation in which the hydrogen-bond length is stochastically modulated in the $v = 0$ and $v = 1$ state with a time constant of 950(100) fs (i.e. diffusion according to Eq. (8.11)), and in which the excited distribution $\Delta n_1(R,t)$ in the $W_1(R)$ potential has an additional rapid shift over a limited distance, directly following its excitation. This shift, which depends on the elapsed time since excitation, cannot easily be incorporated

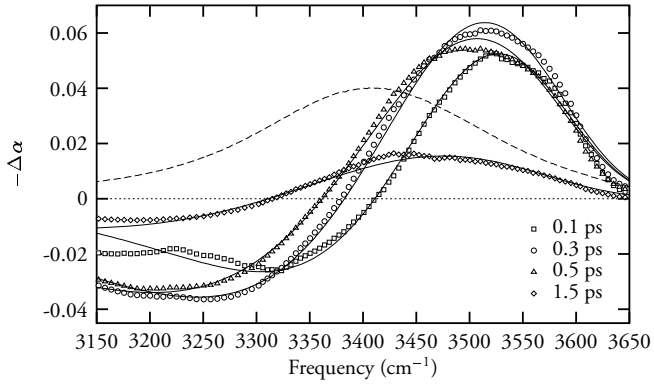

FIGURE 8.7. Transient spectra of HDO:D_2O, pumped at 3580 cm^{-1} at four pump–probe delays. Data points: experiment (by Gallot and co-workers[33,35]); drawn curves: QLS model with inertial shift; dashed curve: linear spectrum of the OH band.

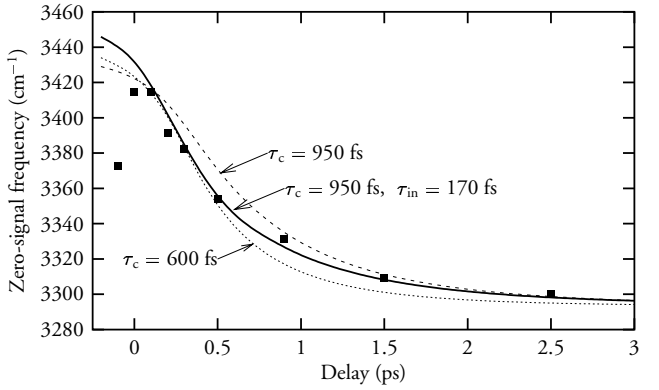

FIGURE 8.8. Frequency at which the bleaching in the transient spectrum changes into an induced absorption as a function of delay. The points were provided by Gallot and co-workers[33,35] who obtained them by exciting the OH stretch vibration in dilute HDO:D_2O at 3580 cm^{-1}. The dashed curves represent calculations in which the hydrogen-bond length is stochastically modulated (diffusion) in the hydrogen-bond potentials W_0 and W_1. The solid curve represents a calculation in which the hydrogen bond is stochastically modulated and in addition experiences a fast shift with a time constant τ_{in} = 170(40) fs towards the minimum of the W_1 potential.

in the time-invariant diffusion equation Eq. (8.11). Therefore, we model the inertial shift phenomenologically in the numerical calculation, with time steps δt and excitation time t_{ex}, with the transformation

$$\Delta n_1(R, t + \delta t) = \Delta n_1(R + \Lambda \delta t, t), \tag{8.12A}$$

$$\Lambda = (S/\tau_{in}) \exp\left((t_{ex} - t)/\tau_{in}\right). \tag{8.12B}$$

In the description of this inertial shift, we incorporated the non-zero pulse duration of the pump and probe pulses. From a fit to the Gallot's transient spectra, we find $S = 0.56(12)$ pm for the total distance over which this shift occurs, and $\tau_{in} = 170(40)$ fs. This value of S corresponds to 45% of the distance between the center of the initially excited hydrogen-bond length distribution and the minimum of the $W_1(R)$ potential.

The presence of a fast initial component in the hydrogen-bond dynamics of the $v = 1$ state can be explained as follows. The oscillation in the hydrogen-bond coordinate R is overdamped, which means that each individual oscillator has a local hydrogen-bond potential that is determined both by the potential W_0 and by the local configuration of the liquid. The excitation with a short pump pulse to the $v = 1$ state leads to a rapid change of W_0 to W_1, and thereby to a change of the local potential. This change of the local potential induces a rapid adaptation of the hydrogen-bond length. For the hole that is burnt in $v = 0$, the local potential does not change, and therefore the dynamics of the hole only result from the diffusive reorganization of the local liquid structure. The presence of a significant fast component in the hydrogen-bond dynamics of liquid water implies that water molecules can adapt to changes in charge distribution or molecular orientation (for instance as a result of chemical reactions) on a time scale that is much shorter than that of the spontaneous reorganization of the liquid.

The time constant $\tau_{in} = 170(40)$ fs of the contraction of the hydrogen-bond length in the $v = 1$ state is much shorter than the time constant $\tau_c = 950(100)$ fs of the spontaneous reorganization of the liquid. This suggests that the fast initial response is a local effect, involving only a few water molecules. Nevertheless, τ_{in} is still much longer than the inverse angular frequency of the undamped OH$\cdots$O hydrogen-bond stretch vibration (the inverse of $\omega = 200$ cm^{-1} is 27 fs).[47] Hence, the fast adaptation of the hydrogen-bond length is still an overdamped motion. The time constant $\tau_{in} = 170$ fs is very similar to that of the fast component of the dielectric relaxation of liquid water that was recently observed with THz reflection spectroscopy.[103,104] This fast dielectric component was also assigned to a local reorganization involving only one or a few water molecules.

8.5 AUTODISSOCIATION OF WATER

The strong delocalization of the $v = 2$ state (Fig. 8.4), especially for hydrogen-bond lengths $R \leq 2.7$ Å, has interesting implications. A direct excitation of the $v = 0 \rightarrow 2$ transition is known to lead to an increased, non-thermal, concentration of H_3O^+ and OH^- ions in pure water. This excess concentration decays on a microsecond time scale due to the recombination of the H_3O^+ and OH^- ions back to water.[40,59] However, the exact mechanism that converted the vibrational energy to a dissociation was not clear. We can now understand this dissociation mechanism from the fact that in the $v = 2$ state, the

hydrogen atom becomes strongly delocalized between the oxygen atoms of two hydrogen-bonded water molecules. The excitation from the localized $v = 0$ ground state to this delocalized $v = 2$ state implies a partial transfer of the hydrogen atom to the other oxygen atom in the $DO{-}H\cdots OD_2$ system. This means that the excitation leads to a high probability for the formation of an oxygen atom to which only one hydrogen is bound and an oxygen atom to which three hydrogen atoms are bound. If this hopping of the hydrogen atom is associated with a charge transfer, not a hydrogen atom but a proton is transfered, which results in the formation of an H_3O^+ ion and an OH^- ion.

Closely related to the above photo-induced dissociation is the (spontaneous) autodissociation reaction

$$HO{-}H\cdots OH_2 \;\rightarrow\; HO^-\cdots HOH_2^+.$$

The rightmost ion, the hydronium ion, exists in ordinary liquid water with a concentration of 10^{-7} mol/l (hence, $pH = 7$). Recent theoretical work[84,37] showed that such an autodissociation will become semi-permanent if the hydronium ion is transported away from the OH^- ion via a Grotthuss conduction mechanism,[♩] in which not the ion itself is transported but rather its charge, along a 'hydrogen-bond wire':

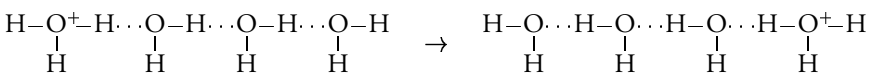

We will now see that the $v = 2$ state of the OH stretch vibration is related to this autodissociation reaction. The first step in the autodissociation of water is the transfer of a proton between two hydrogen-bonded water molecules, a fact that was recently shown by *ab initio* molecular dynamics simulations.[37] However, these simulations do not give information on the (quantum) nature of the transition state of the first proton-transfer step, since they describe the nuclear dynamics classically.

8.5.1 TRANSITION STATE

In the following we will calculate the energy required to induce proton transfer in the $DOH\cdots OD_2$ system formed by an HDO and a D_2O molecule for the different quantum states of the OH stretch vibration. In this calculation, we will use the knowledge from §8.3.1 of the potentials V_I and V_{II}. Proton transfer can occur when the proton has a significant probability amplitude at a distance r_{min} from the right oxygen atom in the $OH\cdots O$ sytem, with r_{min} the equilibrium OH bond length in the $v = 0$ state. This requirement will be fulfilled if the energy of the occupied vibrational state of the OH stretch vibration exceeds $V_I(r, R)$ at $r = R - r_{min}$. Proton transfer can thus be induced by shortening the hydrogen-bond length and/or by exciting the OH stretch vibration to a

[♩] Von Grotthuss,[20] who published his experiments on the electrolysis of salt solutions in 1806, knew about neither protons nor ionic dissociation of salts. He assumed, conforming to the ideas of his time, that in a salt solution, both the water and the salt existed as small neutral particles. He tried to explain the formation of different products at the two electrodes by proposing that each neutral particle consisted of a positive and negative half. Upon electrolysis, salt and water wires would form that extended from cathode to anode, in which a conduction mechanism similar to the above hydronium transport took place. His insight that salts are composed of ions was brilliant, but the 'wire theory' ultimately turned out inaccurate. However, the mechanism for proton and hydroxyl ion transport over short distances, being the only case where the wire theory applies, is named in honor of Von Grotthuss.

TABLE 8.1. Calculated energy $E_{T,v}$ required for proton transfer in a hydrogen-bonded $DOH\cdots OD_2$ system, for the five lowest quantum states v of the O–H stretch vibration and the corresponding distances $R_{eq,o} - R_{T,v}$ over which the hydrogen bond is contracted compared to the ground-state equilibrium value $R_{eq,o} = 2.85$ Å. The strong delocalization of the vibrational states for $v \geq 3$ means that proton transfer can occur without contraction.

quantum number v of transition state	Contraction (pm)	Transition energy (cm^{-1})	(kJ/mol)
0	41	12447	149
1	35	8976	107
2	25	6533	78
3	–	7044	84
4	–	8466	101

delocalized state. To determine the energy required for this transfer in the vibrational state v, we solve $E_v(R) = V_I(R - r_{min}, R)$ for R. The value of R at which this equality holds is denoted as $R_{T,v}$, whose values are shown in Table 8.1. For the higher vibrational states, $R_{T,v} > R_{eq,v}$, which means that the energy $E_v(R)$ already exceeds $V_I(R - r_{min}, R)$ at the equilibrium distance $R_{eq,v}$. The proton transfer energy for state v is: $E_{T,v} = E_v(R_{T,v}) + V_{II}(R_{T,v}) - E_o(R_{eq,o}) - V_{II}(R_{eq,o})$, with $R_{eq,o} = 2.85$ Å. The resulting energies $E_{T,v}$ are shown in Table 8.1.

For the $v = 0$ and $v = 1$ states, the proton transfer requires a strong shortening of the hydrogen bond, which has a high associated energy cost. For the $v = 2$ state, no contraction of the hydrogen bond is required, because of the delocalized character of the proton in this state. The proton is also delocalized in the $v = 3$ and $v = 4$ states, but these states require a larger excitation energy than the $v = 2$ state. Hence, the $v = 2$ state of the OH stretch vibration is the most favorable transition state for getting proton transfer from an HDO molecule to a D_2O molecule. This result agrees with the observation in photolysis experiments that excitation of the $v = 2$ state already suffices to generate a high concentration of non-thermal excess protons and hydroxyl ions.[40,59] The required activation energy $E_{T,2}$ of 6500 cm^{-1} (78 kJ/mol) for autodissociation is less than 20% of the OH binding energy. This illustrates the strong effect of hydrogen bonds on the OH bonds of the water molecule.

For pure H_2O, the interactions between the OH stretch vibrations and the $OH\cdots O$ hydrogen bonds are similar to those in a solution of HDO in D_2O. Therefore, we expect the same qualitative behavior for the mechanism of proton transfer between two H_2O molecules. Quantitatively there will be small differences, because the OH stretch vibrations of the H_2O molecule form delocalized symmetric and asymmetric modes. The energy of the $v = 2$ state of the symmetric mode is lower and that of the asymmetric mode is higher than the energy of the $v = 2$ state of HDO molecule. These energy differences will lead to small changes in the value of the oxygen-oxygen distance $R_{T,2}$ at which proton transfer becomes possible.

The proton-transfer energy $E_{T,2}$ of 6,500 cm^{-1} represents the lowest possible activation energy for proton transfer between two water molecules. This energy is expected to be somewhat higher than the overall enthalpy change ΔH of the autodissociation reaction. ΔH can be calculated using the Van 't Hoff isochore $d \ln K_w / dT = \Delta H / k_B T^2$, with

K_w the autoprotolysis constant of water; $K_w = a(H_3O^+) \cdot a(OH^-) = 1.008 \times 10^{-14}$ at $T = 298$ K, which corresponds to $pH = 7$). From the temperature dependence of K_w,[2] it follows that $\Delta H = 5500$ cm^{-1} (66 kJ/mol) at 298 K, which is approximately 1000 cm^{-1} less than the activation energy $E_{T,2}$, which can be explained from the solvation of the produced H_3O^+ and OH^- ions.

8.5.2 Mechanism

Because the *ab initio* simulations on the autodissociation of water[37] did not describe the motions of the nuclei quantum-mechanically, the present findings provide complementary information on the microscopic mechanism of the autodissociation reaction. This mechanism likely consists of the following steps. (i) Fluctuations of the local water structure lead to excitation of an OH stretch mode to the $v = 2$ state. (ii) This excitation induces a contraction of the hydrogen bond to its new equilibrium length of 2.65 Å (Fig. 8.3). (iii) The contraction leads to a decrease of the barrier in the potential V_1 (Fig. 8.4). The resulting delocalization of the $v = 2$ state enables transfer of the proton to the other (right-hand) oxygen atom. (iv) The proton transfer is followed by a spatial separation of the OH^- and the H_3O^+ ion via proton conduction along the hydrogen-bonded network formed by the surrounding water molecules.[84,118,117] (v) The proton conduction should be followed by a cleavage of the hydrogen-bond network to avoid recombination via the reverse proton-conduction mechanism.[37]

Finally, it should be noted that the hydrogen bonds formed between water and molecules different from water (e.g., dissolved acids and bases) can show a similar effect on the OH stretch frequency as the hydrogen bond between two water molecules. In view of this similarity, we can expect that the proton-transfer reactions between water and these other molecules also proceed via the excited quantum states of the OH stretch vibration. This should be verified in future experimental studies.

8.6 Conclusions

We investigated the transient spectrum of vibrationally excited HDO dissolved in D_2O. The transient absorption ($v = 1 \rightarrow 2$) of the OH stretch mode is strongly asymmetric and much broader than the linear ($v = 0 \rightarrow 1$) absorption spectrum. The shape of the $v = 1 \rightarrow 2$ absorption spectrum can be explained from the strong (anharmonic) interactions between the OH stretch vibration and the OH$\cdots$O hydrogen-bond. These anharmonic interactions are quantitatively described with a quantum-mechanical version of the Lippincott-Schroeder (QLS) model. This model also provides an accurate description of the relations between the hydrogen-bond length, the OH bond length and the OH stretch frequency.

From a detailed study of the transient spectral responses at different delays, we find that the dynamics of the hydrogen-bond length in both the $v = 0$ and the $v = 1$ state of the OH stretch vibration are diffusive processes with a time constant $\tau_c = 950(100)$ fs. These diffusive dynamics result from the spontaneous reorganisations of liquid water. For the $v = 1$ state, the hydrogen-bond dynamics contain an additional fast component with a time constant $\tau_{in} = 170(40)$ fs. This fast component is observed directly after excitation

of the $v = 1$ state out of $v = 0$, and results from the rapid contraction of the hydrogen bond towards its new equilibribrium position in this state.

The wave function of the $v = 2$ state of the OH stretch mode is strongly delocalized, which implies that an excitation to the $v = 2$ state can initiate an autodissociation reaction $2H_2O \rightarrow OH^- + H_3O^+$. The energy required for this excitation is in good agreement with the estimated activation energy for the autodissociation in water.